The Journal of Prevention of Alzheimer's Disease 13 (2026) 100456

Contents lists available at ScienceDirect

The Journal of Prevention of Alzheimer's Disease

journal homepage: www.elsevier.com/locate/tjpad

Synaptic toxicity of OGA inhibitors and the failure of ceperognastat

Jonathan Meade [a], Haylee Mesa [a], Shahriar Alamgir [a], Isabell Bieniecka [a], Lei Liu [*,b], Qi Zhang [**,a]

[a] The Stiles-Nicholson Brain Institute and Department of Chemistry and Biochemistry in College of Science, Florida Atlantic University, Boca Raton, FL, USA
[b] Department of Neurology, Brigham and Women's Hospital, Boston, MA, USA

A B S T R A C T

O-GlcNAcase inhibitors (OGAi) have emerged as a promising therapeutic strategy in Alzheimer's disease (AD) by enhancing O-GlcNAcylation, which competes with tau phosphorylation and reduces tau aggregation. However, the Phase II clinical trial failure of ceperognastat, marked by accelerated cognitive decline in the treatment group, has raised significant safety concerns. Here, we examined the acute synaptic effects of three structurally distinct OGAi compounds—ceperognastat, ASN90, and MK8719—in mouse hippocampal slices. Electrophysiological recordings revealed suppression of both short- and long-term synaptic plasticity, including paired-pulse facilitation/depression and long-term potentiation. Immunohistochemical analysis confirmed disrupted synaptic protein levels (increased PSD-95, reduced Synaptophysin 1) and a biphasic shift in tau phosphorylation. These convergent findings suggest a class-wide synaptotoxic mechanism and call for a great caution in the development of disease-modifying therapies in AD. We argue that preclinical drug screening for synaptic functionality is essential in CNS-targeted therapeutic pipelines.

1. Introduction

Adding O-linked β-N-acetylglucosamine (O-GlcNAcylation) to serine or threonine residues is a reversible post-translational modification in many proteins [1]. This process is regulated by the reciprocal actions of O-GlcNAc transferase (OGT, adding O-GlcNAc) and O-GlcNAcase (OGA, removing O-GlcNAc). Neuronal proteins essential for synaptic transmission and plasticity—including synapsin and AMPA receptors—undergo O-GlcNAcylation [2]. Genetic ablation of OGA causes perinatal lethality, and heterozygous OGA knockout mice exhibit deficits in both long-term potentiation (LTP) and long-term depression (LTD), underscoring the critical role of dynamic O-GlcNAc cycling in neural function [2]. Despite this, OGA became a therapeutic target based on its ability to modulate tau pathology in animal models: O-GlcNAcylation competes with tau phosphorylation, and preclinical studies reported that OGA inhibition reduces tau aggregation [3]. These findings led to the development of OGA inhibitors (OGAi) for Alzheimer's disease and other tauopathies. However, in the Phase II PROSPECT-ALZ trial of the OGAi ceperognastat [4], participants receiving the highest dose (3 mg) exhibited significantly faster cognitive decline than placebo across multiple cognitive measures, raising serious concerns about drug-induced neurotoxicity [5]. This study evaluates whether preclinical synaptic deficits induced by OGAi could have anticipated these adverse outcomes, and whether such effects reflect a class-wide liability for OGA-targeting therapeutics.

2. Methods

2.1. Brain slice preparation

Three OGAi compounds were evaluated: ceperognastat (LY3372689), ASN90 (Egalognastat), and MK8719. All were obtained from MedChem Express. All three OGA inhibitors (OGAi) were stored as 10 mM DMSO solution in −80 °C freezer. Animal use was approved by FAU IACUC (A23–26). All 6-month-old C57B6/J male mice were purchased from the Jackson Laboratory and husbanded in FAU vivarium until use. From those adult mice, 300-μm thick coronal slices containing hippocampal formations were prepared using Leica VT1000S and incubated in recovering artificial cerebrospinal fluid (recovering aCSF, in mM: 92 NaCl, 2.5 KCl, 1.25 NaH_2PO_4, 30 $NaHCO_3$, 20 HEPES, 25 glucose, 2 thiourea, 5 Na-ascorbate, 3 Na-pyruvate, 2 $CaCl_2{\cdot}4H_2O$ and 2 $MgSO_4{\cdot}7H_2O$). During the recovery, DMSO (1:1000 dilution) or 10 μM OGAi (1:1000 dilution from the stock solutions) were applied to the recovery aCSF for ~4h.

2.2. Electrophysiology

All following tests and analyses were done blind. Whole-cell patch-

* Corresponding author at: MGB research building, BLND452, 65 Landsdowne St, Cambridge, MA, 02139, USA.
** Corresponding author at: 5353 Parkside Dr., Florida Atlantic University, Jupiter, FL 33458, USA.
E-mail addresses: lliu35@bwh.harvard.edu (L. Liu), zhangq@health.fau.edu (Q. Zhang).

https://doi.org/10.1016/j.tjpad.2025.100456
Received 8 September 2025; Received in revised form 25 October 2025; Accepted 16 December 2025
Available online 1 January 2026

clamp recording of CA1 neurons was performed in the recording aCSF (in mM: 119 NaCl, 2.5 KCl, 1.25 NaH_2PO_4, 24 $NaHCO_3$, 12.5 glucose, 2 $CaCl_2{\cdot}4H_2O$ and 2 $MgSO_4{\cdot}7H_2O$) with the same concentrations of DMSO or OGAi as those during recovery. Schaffer collateral stimulations for paired-pulse facilitation and depression (30 Hz 0.15 s, *i.e.*, 5 pulses per episode and five episode with 10-second interval in between) and long-term potentiation (100-Hz 1-second tetanus stimulation) were delivered via a micro-electrode. For EPSC, membrane potentials were held between −70 and −40 mV). All experiments were performed using ROE-200 dual-manipulator and MPC-200 controller (Sutter Instruments), MultiClamp 700B and DigiData 1440A controlled by pCLAMP 10 (Molecular Devices). Clampfit 10.6 was used for data analysis and extraction.

2.3. Immunocytochemistry

After recording, slices were fixed using 4 % paraformaldehyde in phosphate-buffered saline (PBS, in g for 1 L, 8 NaCl, 0.2 KCl, 1.15 $Na_2HPO_4{\bullet}7H_2O$, 0.2 KH_2PO_4, pH = 7.35) for 1 hour at room temperature. The fixation and all subsequent steps were carried out in 12-well plates and on a plate shaker rotating at 60 rpm. After three times wash with PBS, slices were permeabilized with 3 % Triton X-100 (in PBS) for 1 hour and blocked by 5 % Goat serum (Abcam), 5 % (W/V) protease-free BSA (W/V) and 0.25 % Triton X-100 (in PBS) for 1 hour at room temperature. Primary antibody combos (Table S1) were prepared in fresh block solution and incubated with those slices at 4 °C overnight. After the removal of primary antibodies, the slices were washed three times with PBS containing 5 % Goat serum, 0.5 % (W/V) protease-free BSA (W/V) and 0.25 % Triton X-100. The secondary antibody combos (Table S2) were applied in the same solution for 4 h at room temperature. After the removal of secondary antibody, slices were stained with Hoechst 33,342 nucleic acid stain (Invitrogen) for 30 min at room temperature and washed with PBS and Milli-Q water twice for each. All slices were mounted in VECTASHIELD® antifade mounting media (Vector Laboratories).

2.4. Image acquisition and analyses

Multichannel confocal images of those brain slices were acquired using a Nikon A1R laser scanning confocal microscope equipped with a Nikon Plan Apo VC 20X N.A. 0.75 objective and controlled by NIS-Elements AR (Version 5.42.04). The acquisition settings are as follows: DAPI (*i.e.*, Hoechst 33,342), 405 nm for excitation, 430-475 nm for emission, 1.0 for laser power, 60 for gain, 17.88 μm pinhole size; CF488A®, 488 nm, 500-550 nm, 0.3, 80, 26.82 μm; CF568®, 560 nm, 570-616 nm, 3.0, 80, 26.82 μm; CF647®, 641 nm, 660-710 nm, 5.0, 90, 26.82 μm. With such settings, the pixel intensities corresponding to biological specimens never exceeded the dynamic range of 10-bit image (*i.e.*, 0 – 4095). Z-stack step size is 3 μm.

All images were imported into FIJI (ImageJ2) by Bio-Formats (plug-in). For every brain slice, three Z-consecutive sections in the middle of the image stack were projected along z-axis using their average pixel intensities. For analysis, hippocampal formations were selected from the project images. Within every image, four cell-free regions of interest (ROIs) were selected, and the mean as well as the standard deviation of their pixel intensities for every channel were calculated to determine the background fluorescence intensity. ROI selection in individual channel was done by thresholding, which was set at 3 times of standard deviation above the mean background pixel intensities. For postsynaptic PSD95, Tuj1-positive, GFAP- and DAPI-negative ROIs were generated via Boolean operations of all three corresponding images. Similar operations were done to generate ROIs for Synaptophysin 1 and pTau (*i.e.*, Tau-positive and DAPI-negative). Next, the average pixel intensity of every ROI was calculated and imported into Excel spreadsheet, in which it was subtracted by the average pixel intensity of the background ROIs in the same image. All resulting intensity values were randomized and 111 of them for every brain slice were used for statistical analyses in Prism (10.2.3, GraphPad).

2.5. Statistics

In every electrophysiological test, we used data from all 9 neurons in nine brain slices (one per slice) prepared from three mice (three slice per mouse) for every treatment (*i.e.*, DMSO and three OGAi). We first used Welch's ANOVA test to determine if there were any significance differences across all four treatments. Then, we used Kolmogorov-Smimov test to compare every OGAi treatment with DMSO control. The violin plot in Fig. 1C represented the average value for every neuron for 60-90 s whereas the main plot represented the averages and the standard deviations of data points from all 9 neurons at every time point. For immunofluorescence comparison, we used all 9 slices and performed Welch's ANOVA test followed by Kolmogorov-Smimov test to compare individual OGAi with DMSO control.

3. Results

We assessed short-term synaptic plasticity by measuring paired-pulse facilitation (PPF) and depression (PPD) in mouse hippocampal slices treated with 10 μM OGAi or DMSO for 4 h. PPF was defined as the response increase across five pulses in the first stimulation episode (Figure 1A1), and PPD as the reduction in the first response across five episodes (Figure 1A2). All three OGAi reduced both PPF and PPD compared to control (Fig. 1B), indicating impaired presynaptic plasticity. Next, we evaluated long-term potentiation (LTP) and found that all OGAi significantly suppressed LTP induction (Fig. 1C). These results demonstrate that OGAi from three distinct pipelines disrupt both short- and long-term synaptic plasticity, implying pre- and postsynaptic alternation.

To further assess synaptic changes following acute OGAi treatment, we performed immunohistochemistry using well-validated antibodies (Tables S1 and S2). We observed a significant increase in PSD-95 immunolabeling within Tuj1-positive and GFAP-negative regions (Fig. 2A & C). Additionally, OGAi reduced Synaptophysin 1 labeling in Tau-positive neurites (Fig. 2B & D). Together, these findings demonstrate that OGAi induces morphological changes in both dendritic and axonal compartments. As of Tau, OGAi exposure did decrease its average phosphorylation with an increase of variability (Fig. 2E), affirming their intended inhibition of O-GlcNAcylation. Given the functional roles of Synaptophysin 1 and PSD-95, it is clear that crucial steps of neurotransmission like the secretion and the detection of neurotransmitters can be affected by OGAi, which matches the electrophysiological changes we observed.

4. Discussion

Ceperognastat's failure echoes the repeated clinical disappointments of BACE inhibitors (BACEi), shown to impair cognitive function through acute disruption of neurotransmission [7]. Although mechanistically distinct, both drug classes share a common outcome: BACEi impair synaptic function by prolonging the half-life of cleavable synaptic substrates, while OGAi disrupt synaptic integrity by stagnating synaptic protein O-GlcNAcylation. While we recognize the testing concentrations for the OGAis' are on the high end and we could not exclude potential additive effect of stimulations on OGAi, our findings serve as a cautionary tale for ongoing OGAi programs and future drug development efforts targeting chronic cognitive or neurological disorders. We strongly advocate for the routine incorporation of electrophysiological assessments into toxicology panels to identify synaptic liabilities before advancing compounds into clinical trials. In this study, we investigated the synaptic consequences of OGAi administration, reportedly achieving > 95 % OGA enzyme occupancy[4]—levels that in hindsight reflect a fundamentally flawed therapeutic strategy for a treatment of chronic

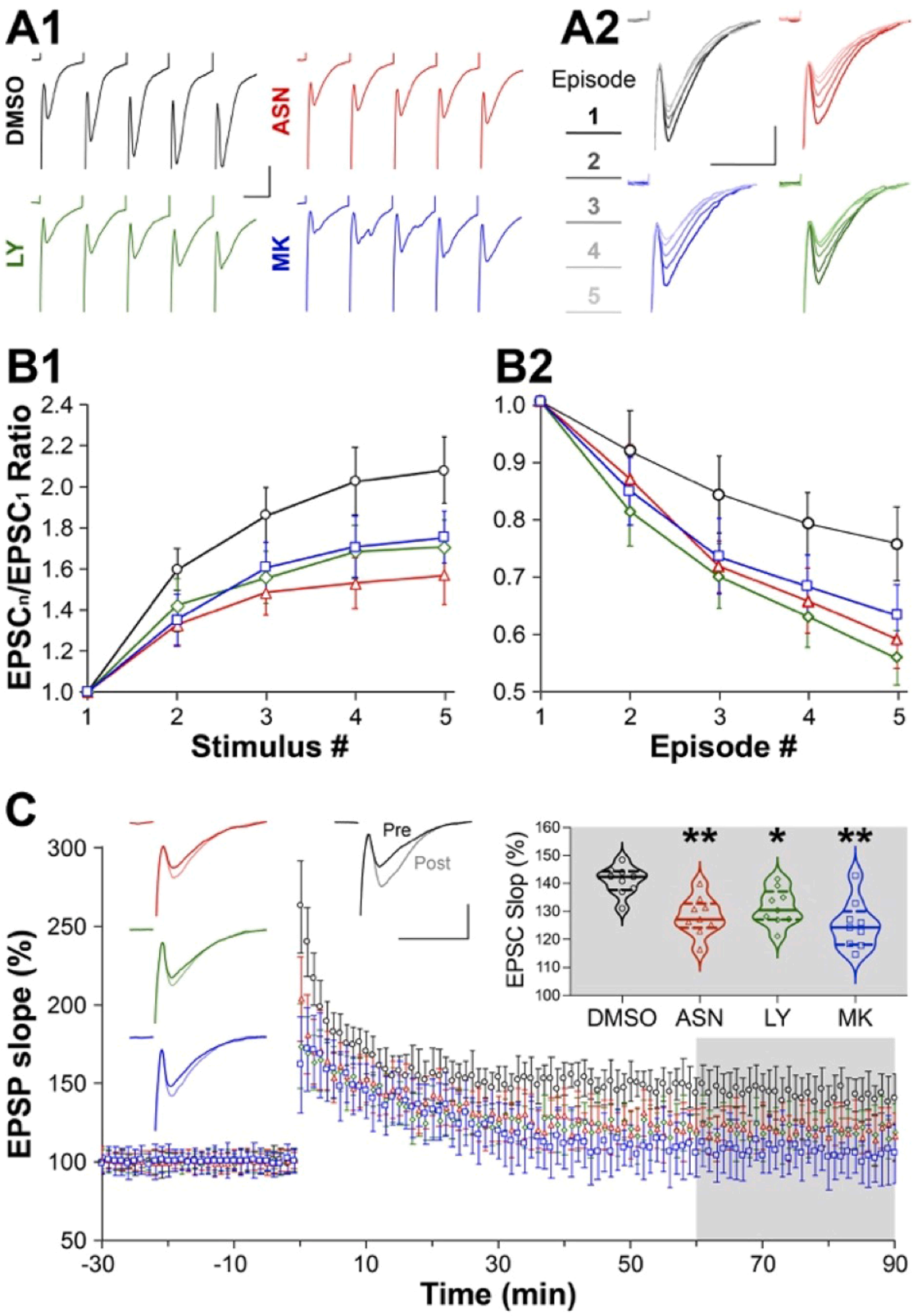

Fig. 1. OGA inhibitors alter synaptic plasticity.
A, sample traces of whole-cell patch clamp recording of hippocampal CA1 pyramidal neurons during the first episode of paired-pulse stimulation (**A1**) and aligned first response from every episode (**A2**). Scale bar, 20 ms (horizontal) and 0.5pA (vertical). The color coding for DMSO (black), ASN90 (*i.e.*, ASN, red), LY3372689 (*i.e.*, LY, green), and MK8719 (*i.e.*, MK, blue) is used in all plots. **B**, plots of EPSC ratio for the responses during the first episode (**B1**) and the first responses of five episodes (**B2**). **C**, LTP measured as relative EPSP slopes after the treatments of OGAi or DMSO. Left insets are sample traces pre- and post 100-Hz 1-s tetanus stimulation. Right inset is a violin plot of the average values during the last 30-s recording (*i.e.*, gray box in the plot). Welch's ANOVA test, W (DFn, DFd) = 10.61 (3.000, 17.50), $p = 0.0003$; Kolmogorov-Smimov test, $p = 0.0063$ (ASN *vs.* DMSO), 0.0336 (LY *vs.* DMSO), and 0.0063 (MK *vs.* DMSO). $N = 3$ mice and $n = 3$ slices (*i.e.*, 9 recordings in total for every treatment). *, $0.05 > p \geq 0.01$; **, $0.01 > p \geq 0.005$; ***, $0.005 > p \geq 0.001$, ****, $p < 0.001$.

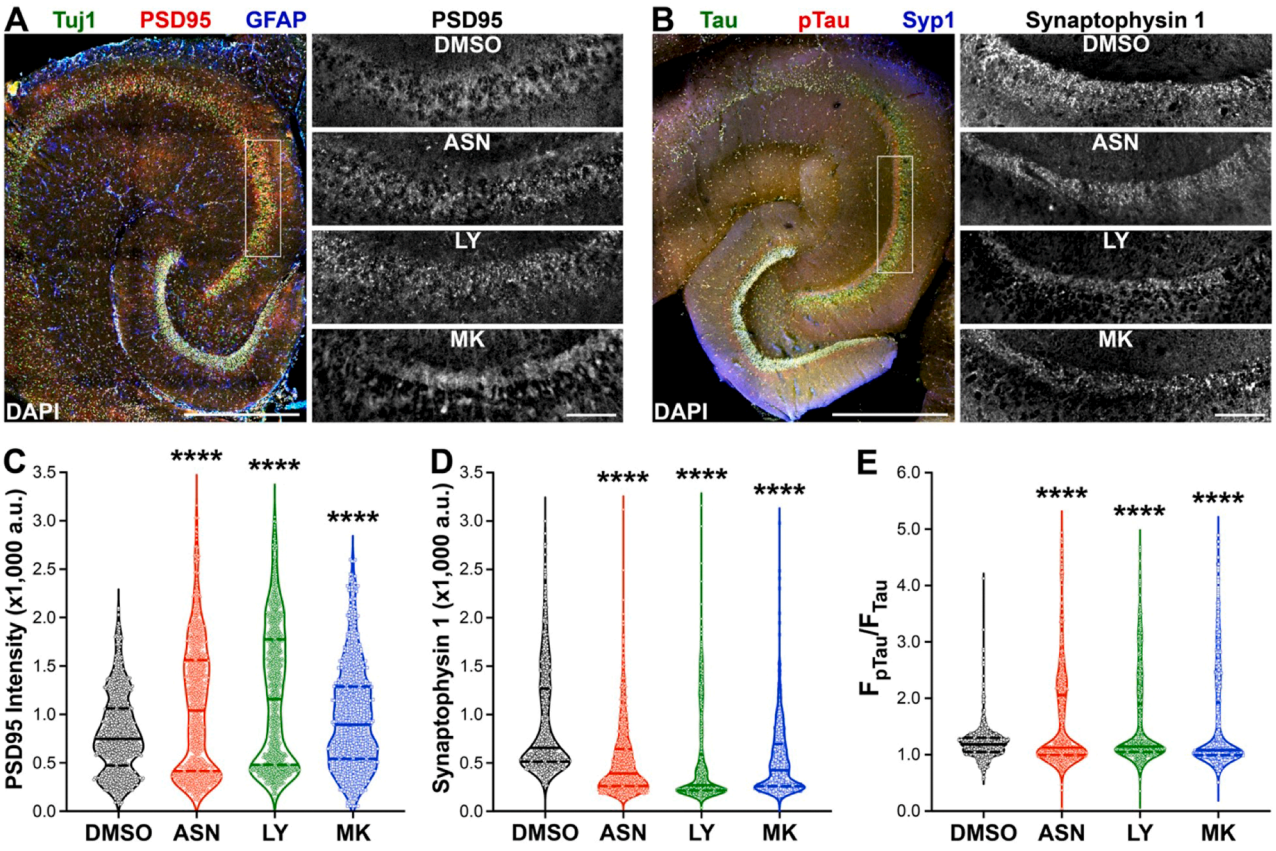

Fig. 2. OGA inhibitors alter synaptic protein levels and Tau phosphorylation.
A, sample images of fluorescence immunocytochemistry for PSD95, Tuj1, GFAP, and DAPI. Scale bar, 0.5 mm. Images on the left are zoom-in images of PSD95 immunofluorescence in the cell-body layer (indicated by the white box) for all four treatments. Scale bar, 50 μm **B**, sample images of fluorescence immunocytochemistry for Synaptophysin 1, Tau, pTau, and DAPI. Images on the left are zoom-in images of Synaptophysin 1 immunofluorescence in the cell-body layer (indicated by the white box) for all four treatments. **C**&**D**, violin plots of PSD95 (**C**) and Synaptophysin 1 (**D**) immunofluorescence intensities. **E**, violin plots of pTau *vs.* Tau fluorescence intensity (F) ratios from the same ROIs of Synaptophysin 1. Welch's ANOVA test for PSD95, W (DFn, DFd) = 90.96 (3.000, 2168), $p < 0.0001$; for Synaptophysin 1 fluorescence intensity, W (DFn, DFd) = 153.30 (3.000, 2187), $p < 0.0001$; for pTau/Tau, W (DFn, DFd) = 128.40 (3.000, 1918), $p < 0.0001$. Kolmogorov-Smimov test for all three, $p < 0.0001$ (ASN *vs.* DMSO, LY *vs.* DMSO, and MK *vs.* DMSO). $N = 9$ slices from 3 mice (3 ea), $n = 999$ ROIs (111 randomly selected from every slice). *, $0.05 > p \geq 0.01$; **, $0.01 > p \geq 0.005$; ***, $0.005 > p \geq 0.001$, ****, $p < 0.001$.

neurological cognitive diseases. As Biogen's Phase I BIIB113 study [6] highlighted, potential impacts on synaptic transmission should be considered in the design and interpretation of clinical OGA inhibitor programs. Further mechanistic study is needed to understand the molecular underpinnings of this drug-induced cognitive decline and to prevent similar adverse outcomes in future clinical programs.

Conflict of interest disclosure

Drs. Liu, Zhang report grants from National Institute on Aging during the conduct of the study. No other disclosures were reported.

Funding

This work was funded by National Institutes of Health grants RF1 AG079569, R01AG071865, and R15 AG085620, and Florida Department of Health grants 21A04 and 24A03. The funders had no role in data collection, analysis, or publication decisions.

Acknowledgements

We thank Dr. Hideki Iwamoto for helping with adult brain slice preparation.

CRediT authorship contribution statement

Jonathan Meade: Investigation. **Haylee Mesa:** Investigation. **Shahriar Alamgir:** Writing – review & editing. **Isabell Bieniecka:** Writing – review & editing. **Lei Liu:** Writing – review & editing, Writing – original draft, Supervision, Investigation, Funding acquisition, Conceptualization. **Qi Zhang:** Writing – review & editing, Writing – original draft, Visualization, Supervision, Resources, Project administration, Investigation, Funding acquisition, Formal analysis, Data curation, Conceptualization.

Declaration of competing interest

The authors declare that they have no known competing financial interests or personal relationships that could have appeared to influence the work reported in this paper.

Supplementary materials

Supplementary material associated with this article can be found, in the online version, at doi:10.1016/j.tjpad.2025.100456.

References

[1] He M, Zhou X, Wang X. Glycosylation: mechanisms, biological functions and clinical implications. Sig Transduct Target Ther 2024;9(1):1–33. https://doi.org/10.1038/s41392-024-01886-1.

[2] Yang YR, Song S, Hwang H, et al. Memory and synaptic plasticity are impaired by dysregulated hippocampal O-GlcNAcylation. Sci Rep 2017;7(1):44921. https://doi.org/10.1038/srep44921.

[3] Hastings NB, Wang X, Song L, et al. Inhibition of O-GlcNAcase leads to elevation of O-GlcNAc tau and reduction of tauopathy and cerebrospinal fluid tau in rTg4510 mice. Mol Neurodegener 2017;12(1):39. https://doi.org/10.1186/s13024-017-0181-0.

[4] Kielbasa W, Goldsmith P, Donnelly KB, et al. Discovery and clinical translation of ceperognastat, an O-GlcNAcase (OGA) inhibitor, for the treatment of Alzheimer's disease. Alzheimer's Dement: Transl Res Clin Interv 2024;10(4):e70020. https://doi.org/10.1002/trc2.70020.

[5] 17th Clinical Trials on Alzheimer's Disease (CTAD). Madrid, Spain, October 29 - November 1, 2024: conference proceedings. J. Prev Alzheimer's Dis 2025;12(1 Supplement):100043. https://doi.org/10.1016/j.tjpad.2024.100043.

[6] Nery FC, Kaliszczak M, Suttle B, et al. Results of the first-in-human, randomized, double-blind, placebo-controlled, single- and multiple-ascending dose study of BIIB113 in healthy volunteers. J Preven Alzheimer's Dis July 2025:100302. https://doi.org/10.1016/j.tjpad.2025.100302. Published online.

[7] Li S, Liu L, Selkoe D. Verubecestat for prodromal Alzheimer's disease. N Engl J Med 2019;381(4):388–9. https://doi.org/10.1056/NEJMc1906679.